

Production and detection of atomic hexadecapole at Earth's magnetic field

V. M. Acosta,¹ M. Auzinsh,² W. Gawlik,³ P. Grisins,² J. M. Higbie,¹
D. F. Jackson Kimball,⁴ L. Krzemien,³ M. P. Ledbetter,¹ S. Pustelny,³
S. M. Rochester,¹ V. V. Yashchuk,⁵ D. Budker^{1,6*}

¹*Department of Physics, University of California Berkeley, CA 94720-7300*

²*Department of Physics, University of Latvia, 19 Rainis Blvd, Riga, LV-1586, Latvia*

³*Center for Magneto-Optical Research Institute of Physics, Jagiellonian University
Reymonta 4, 30-059 Kraków, Poland*

⁴*Department of Physics, California State University –East Bay 25800 Carlos Bee
Blvd., Hayward, CA 94542, USA*

⁵*Advanced Light Source Division, Lawrence Berkeley National Laboratory,
Berkeley CA 94720, USA*

⁶*Nuclear Science Division, Lawrence Berkeley National Laboratory, Berkeley CA
94720, USA*

**To whom correspondence should be addressed;*

budker@berkeley.edu

Abstract: Optical magnetometers measure magnetic fields with extremely high precision and without cryogenics. However, at geomagnetic fields, important for applications from landmine removal to archaeology, they suffer from nonlinear Zeeman splitting, leading to systematic dependence on sensor orientation. We present experimental results on a method of eliminating this systematic error, using the hexadecapole atomic polarization moment. In particular, we demonstrate selective production of the atomic hexadecapole moment at Earth's magnetic field and verify its immunity to nonlinear Zeeman splitting. This technique promises to eliminate directional errors in all-optical atomic magnetometers, potentially improving their measurement accuracy by several orders of magnitude.

© 2008 Optical Society of America

OCIS codes: (020.1670) Coherent optical effects; (020.4180) Multiphoton processes; (210.3810) Magneto-optic systems

References and links

1. J. Vanier and C. Audoin, *The quantum physics of atomic frequency standards* (A. Hilger, Bristol; Philadelphia, 1989).
2. D. Budker and M. V. Romalis, "Optical Magnetometry," *Nature Phys.* **3**, 227–234 (2007).
3. P. S. J. Ivan H. Deutsch, Gavin K. Brennen, "Quantum Computing with Neutral Atoms in an Optical Lattice," *Fortschritte der Physik* **48**, 925–943 (2000).
4. B. Julsgaard, J. Sherson, J. I. Cirac, J. Fiurasek, and E. S. Polzik, "Experimental demonstration of quantum memory for light," *Nature* **432**, 482–486 (2004).
5. G. Yusa, K. Muraki, K. Takashina, K. Hashimoto, and Y. Hirayama, "Controlled multiple quantum coherences of nuclear spins in a nanometre-scale device," *Nature* **434**, 1001–1005 (2005).
6. E. B. Alexandrov, "Recent Progress in Optically Pumped Magnetometers," *Phys. Scr.* **T105**, 27–30 (2003).
7. I. K. Komins, T. W. Kornack, J. C. Allred, and M. V. Romalis, "A subfemtotesla multichannel atomic magnetometer," *Nature* **422**, 596–599 (2003).
8. V. V. Yashchuk, D. Budker, W. Gawlik, D. F. Kimball, Y. P. Malakyan, and S. M. Rochester, "Selective addressing of high-rank atomic polarization moments," *Phys. Rev. Lett.* **90**, 253,001 (2003).

9. S. Pustelny, D. F. Jackson Kimball, S. M. Rochester, V. V. Yashchuk, W. Gawlik, and D. Budker, "Pump-probe nonlinear magneto-optical rotation with frequency-modulated light," *Phys. Rev. A* **73**, 023,817 (2006).
10. G. Xu and D. J. Heinzen, "State-selective Rabi and Ramsey magnetic resonance line shapes," *Phys. Rev. A* **59**, R922–R925 (1999).
11. D. Heinzen and G. Xu, "Application of quantum control theory to manipulate the Zeeman states of an atom," *Quantum Electronics and Laser Science Conference Technical Digest*. 177–178 (1999).
12. C. Chin, V. Leiber, V. Vuletić, A. J. Kerman, and S. Chu, "Measurement of an electron's electric dipole moment using Cs atoms trapped in optical lattices," *Phys. Rev. A* **63**, 033,401 (2001).
13. A. K. V. E. B. Aleksandrov, M. V. Balabas, and A. S. Pazgalev, "Multiple-quantum radio-frequency spectroscopy of atoms: Application to the metrology of geomagnetic fields," *J. Tech. Phys.* **44** (1999).
14. E. B. Alexandrov, A. S. Pazgalev, and J. L. Rasson, "Observation of four-quantum resonance in the Zeeman structure of the ground-state of ^{39}K ," *Opt. Spectrosk.* **82**, 14–20 (1997).
15. A. I. Okunevich, "On the possibility of detecting the transverse component of the hexadecapole moment of atoms in fluorescent emission," *Opt. Spectrosk.* **91**, 177–83 (2001).
16. A. Omont, *Irreducible Components of the Density Matrix: Application to Optical Pumping* (Pergamon Press, 1977).
17. M. Auzinsh, "Angular momenta dynamics in magnetic and electric field: classical and quantum approach," *Can. J. Phys.* **75**, 853–72 (1997).
18. S. M. Rochester and D. Budker, "Atomic polarization visualized," *Am. J. Phys.* **69**, 450–4 (2001).
19. E. B. Alexandrov, M. Auzinsh, D. Budker, D. F. Kimball, S. M. Rochester, and V. V. Yashchuk, "Dynamic effects in nonlinear magneto-optics of atoms and molecules: review," *J. Opt. Soc. Am. B* **22**, 7–20 (2005).
20. E. B. Alexandrov, M. V. Balabas, D. Budker, D. English, D. F. Kimball, C. H. Li, and V. V. Yashchuk, "Light-induced desorption of alkali-metal atoms from paraffin coating," *Phys. Rev. A* **66**, 042,903/1–12 [Erratum: *Phys. Rev. A* **70**, 049,902(E) (2004)] (2002).
21. V. Acosta, M. P. Ledbetter, S. M. Rochester, D. Budker, D. F. Jackson-Kimball, D. C. Hovde, W. Gawlik, S. Pustelny, and J. Zachorowski, "Nonlinear magneto-optical rotation with frequency-modulated light in the geophysical field range," *Phys. Rev. A* **73**, 053,404 (2006).
22. G. W. Series, "Theory of the modulation of light in optical pumping experiments," *Proc. Phys. Soc.* **88**, 957–968 (1966).
23. M. Ducloy, "Nonlinear effects in optical pumping of atoms by a high-intensity multimode gas laser. General theory," *Phys. Rev. A* **8**, 1844–59 (1973).
24. M. P. Auzinsh, M. Y. Tamanis, and R. S. Ferber, "Zeeman quantum beats after optical depopulation of the ground electronic state of diatomic molecules," *Sov. Phys. JETP* **63**, 688–693 (1986).
25. S. Pustelny, D. F. Jackson Kimball, S. M. Rochester, V. V. Yashchuk, and D. Budker, "Influence of magnetic-field inhomogeneity on nonlinear magneto-optical resonances," *Phys. Rev. A* **74**, 063,406 (2006).

1. Introduction

Coherent quantum superpositions of atomic spin states are an essential ingredient of precision measurement devices such as atomic clocks and optical magnetometers [1, 2], and are the workhorse of leading proposals to implement a quantum computer [3, 4]. Radiofrequency and optical radiation are powerful tools for creating, manipulating, and probing these states. However, absorption and emission of single photons, which carry one unit of spin angular momentum, can only create or probe coherences between states differing by at most two spin quanta, whereas ground-state alkali atoms support four-quantum to eight-quantum coherences, depending on the value of the nuclear spin. As a result, only a reduced manifold of the available quantum state-space in such systems can be efficiently manipulated by conventional, low-power optical techniques. Higher-order coherences can be produced and probed by multiple-photon interactions, but often with high optical power requirements, increased relaxation, and population of undesired states. Control over the full range of many-quantum atomic coherences represents an important scientific goal, with significant applications to storage of quantum information and precision magnetic-field sensors.

A complication in the manipulation of high-order coherences arises when the energies of spin states are non-uniformly spaced. Such non-uniform splittings arise in a variety of contexts, including nonlinear Zeeman (NLZ) splitting of alkali ground-state levels at Earth's magnetic field, splittings of nuclear-spin energy levels under the influence of electric-field gradients in a crystal [5], and Stark shifts of atomic states by static or oscillating electric fields. In Earth-

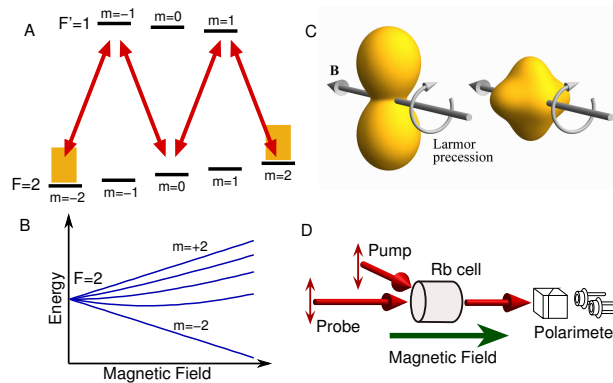


Fig. 1. States, energies, and layout of experiment. Part A shows the states involved in the four-quantum coherence. Part B shows the linearity of the $m = \pm 2$ states' energies as a function of magnetic field (shown for purposes of illustration over a much larger range of fields than are experimentally relevant). Part C shows angular momentum probability surfaces (see text) for quadrupole (left) and hexadecapole (right) for $F = 2$. The atomic polarizations are transverse to and precess around the magnetic-field quantization axis. Part D shows the respective directions of laser polarizations (two-headed arrows), propagation directions, and magnetic field.

field atomic magnetometry, for example, the NLZ splitting leads to split or poorly resolved resonances, resulting in reduced signals and so-called heading errors, i.e., errors in the magnetometer reading that depend on its orientation. Such errors are typically on the nanotesla scale, far larger than the femtotesla-scale sensitivity achievable with atomic magnetometers [6, 7].

Prior work using nonlinear magneto-optical techniques demonstrated selective production and detection of higher polarization moments (as defined in section 2) in the ground states of the alkali atoms [8, 9] but employed techniques not applicable at Earth's field. The production of $\Delta m = 8$ coherences in laser-cooled cesium, where m is the spin projection quantum number, by radiofrequency techniques has been demonstrated by Xu et al. [10] and refined by the same authors [11] using techniques of quantum control theory. Chin et al. have proposed an alternative method of creating $\Delta m = 4$ coherences using a single Rabi pulse from a pair of Raman laser beams applied to an $m = 0$ initial state in ultracold cesium [12]. Aleksandrov et al. have moreover studied four-quantum radiofrequency resonances in potassium with respect to precision magnetometry [13]. In contrast, the present work presents an all-optical technique using a sample of room-temperature atoms suitable for practical optical magnetometry.

To address the significant technological problem of eliminating heading error in optical or atomic magnetometers, we have developed a method that allows selective creation of a long-lived ground-state four-quantum coherence at Earth's field. The energy levels and optical transitions involved are illustrated in Fig. 1(a). Because the hexadecapole moment involves states whose energy as a function of magnetic field is strictly linear (see Fig. 1(b)), it is expected to show no NLZ shifts [14, 15]. As a consequence of having only a single resonant frequency, a practical hexadecapole-based magnetometer would be a better "scalar" magnetometer – it would register the same magnetic field regardless of its spatial orientation. We experimentally demonstrate the immunity of the hexadecapole signal to NLZ splitting using total spin $F = 2$ ^{87}Rb atoms.

2. Theoretical background

Anisotropy of atomic states is characterized by population differences and coherences between Zeeman sublevels. The symmetry properties of such states are conveniently described in terms of polarization moments (PMs) [16]. Polarization moments characterizing anisotropy of a state with total angular momentum F are coefficients in the expansion of the density matrix into irreducible tensor operators of rank $\kappa = 0, \dots, 2F$ and projection $q = -\kappa, \dots, \kappa$. The lowest PMs are population ($\kappa = 0$), orientation ($\kappa = 1$), and alignment ($\kappa = 2$). Mathematically, the polarization moments are given by

$$\rho_q^{(\kappa)} = \sum_{m,m'=-F}^F (-1)^{F-m'} \langle F, m, F, -m' | \kappa q \rangle \rho_{m,m'}. \quad (1)$$

The atomic hexadecapole ($\kappa = 4$) has nine independent components, of which two (those with $q = \pm 4$) are of particular importance for the present work. From Eq. (1), these components are given in terms of those of the density matrix by

$$\begin{aligned} \rho_{+4}^{(4)} &= \rho_{2,-2} \\ \rho_{-4}^{(4)} &= \rho_{-2,2}. \end{aligned}$$

These spherical components evolve in time as $e^{\pm 4i\Omega_L t}$; physically measurable signals are then proportional to the real-valued sum and difference of these components, i.e., to $\rho_{+4}^{(4)} + \rho_{-4}^{(4)}$ and to $i\rho_{+4}^{(4)} - i\rho_{-4}^{(4)}$. It is superpositions such as these of the two extremal states of the hexadecapole multiplet that are produced and detected in this work.

Polarization moments can be illustrated by polarization probability surfaces [17, 18, 19], in which the distance between the origin and the surface in a given direction is proportional to the probability of finding maximal projection $m = F$ in that direction. Fig. 1(b) in the main text shows such surfaces for the quadrupole ($\kappa = 2$) and hexadecapole ($\kappa = 4$) moments. Polarization probability surfaces illustrating the symmetries of the polarization moments under study are shown in Fig. 1(c). In a magnetic field, the atomic angular momentum precesses at the Larmor frequency Ω_L , which is proportional to the applied field. Consider the ‘‘peanut’’-shaped quadrupole moment of Fig. 1(c). When the peanut has rotated by an angle π , it is impossible to differentiate it from its initial state, i.e., it has a twofold symmetry. Consequently, efficient pumping of the quadrupole is achieved with light modulated at an angular frequency $2\Omega_L$. Precession of the quadrupole results in optical rotation of an incident probe beam oscillating at $2\Omega_L$. Similarly, precession of the hexadecapole results in a rotation signal at $4\Omega_L$. More generally, a PM with a component q has $|q|$ -fold symmetry and can therefore be pumped with light harmonically modulated at $|q|\Omega_L$ or with pulses at a repetition rate of $|q|\Omega_L/(2\pi n)$, where n is an integer. The polarization moments prepared in this way produce an optical rotation signal at $|q|\Omega_L$ [9, 8].

3. Experimental setup

The experimental geometry for the measurements presented here is pictured in Fig. 1(d). A New Focus Vortex diode laser tuned to the ^{87}Rb $F = 2 \rightarrow F' = 2$ transition on the D1 (795 nm) line was separated into two beams: a 4-mW linearly polarized pump beam that was amplitude-modulated by electronically varying the 80 MHz radiofrequency power delivered to an acousto-optic modulator (AOM), and a continuous probe beam with the same initial polarization. The probe power was 25 μW for the data shown in Figs. 2 and 3 and 9 μW for the data shown in Fig. 4. The laser frequency was fine-tuned to maximize the hexadecapole signal. Additional

data were taken with a single laser beam serving as both pump and probe, tuned to the $F = 2 \rightarrow F' = 1$ transition. The Rb atoms were contained in an evacuated glass cell with paraffin antirelaxation coating [20]. The cell was enclosed in an oven that maintained the cell at 42°C . Four layers of μ -metal shielding and a multi-order gradient-coil system were used to maintain a stable magnetic field of 510 mG ($51\ \mu\text{T}$). The angle of polarization of the outgoing probe beam was measured using a Rochon polarizing beam splitter and a pair of high-speed, large area photodiodes.

Atomic magnetometers operate by producing transverse atomic polarization and optically detecting its precession in a magnetic field [2]. In our experiments, the $F = 2$ ground-state atoms were pumped using a sequence of short pulses of linearly polarized light with a repetition rate determined by the Larmor precession frequency of the atomic angular momentum. At the end of the sequence, the pump light was blocked. The evolution of the atomic polarization was observed by measuring the angle of optical rotation of an unmodulated probe beam whose initial polarization was the same as that of the pump. We modulated the pumping light at a frequency which approximately matched the Larmor frequency at the applied field, and this field was then determined precisely by measuring the frequency of the optical-rotation signal.

4. Results and discussion

Pumping at a rate $4\Omega_L$ creates a hexadecapole moment without an accompanying transverse quadrupole moment [8, 9]. This is desirable, as the presence of the typically much larger quadrupole signal makes it difficult to observe the hexadecapole. Unfortunately, the amount of hexadecapole pumped in this way rapidly decreases with the magnetic field strength, as seen in Fig. 2 (filled red squares). This can be understood by noting that angular-momentum conservation requires participation of two photons to produce the atomic hexadecapole. When pumping at $4\Omega_L$, both photons must interact with the atoms within the same pulse in order to create the hexadecapole, since separate single-photon processes occurring during successive pumping cycles create quadrupole moments that are orthogonal to each other. This orthogonality is a result of Larmor precession by $\pi/2$ radians in one pumping period. Thus, the quadrupole polarizations from successive cycles cancel the transverse quadrupole, and the net result is a longitudinal quadrupole, seen as a “doughnut” in the inset of Fig. 3, which does not aid in the creation of transverse hexadecapole. As the field increases, the pumping period [$T = 2\pi/(4\Omega_L)$] decreases, reducing the probability of a process occurring which involves interactions with two photons in a single pulse. Even using the strongest pump power available in the experiment (4 mW), the hexadecapole signals cannot be distinguished above noise at the Earth’s field ($4\Omega_L/2\pi \approx 1.4$ MHz) in this scheme.

An alternative method for efficiently pumping the hexadecapole moment is to use light modulated at $2\Omega_L$, producing both quadrupole and hexadecapole moments. In this scheme, the requirement of pumping the hexadecapole in a single pulse is alleviated as the hexadecapole can be obtained by “promoting” the quadrupole polarization with just a single-photon interaction. This method allows one to obtain hexadecapole signals that, while still decreasing with magnetic field in the present experiment, nevertheless remain observable at the Earth’s field (Fig. 2). Both hexadecapole and quadrupole signals decrease as a function of magnetic field, the hexadecapole because it requires a two-photon probing step to occur in an ever-decreasing time interval, and the quadrupole because we use the same high probe-laser power for both signals in order to compare them directly. This decrease of hexadecapole signal is qualitatively reproduced by a model density-matrix calculation. We additionally verified that the quadrupole signal did not drop for magnetic fields up to 268 mG when we instead used a low probe-light power of $3\ \mu\text{W}$.

Figure 3 (top) shows the optical rotation signal obtained with 1500 square pump pulses with

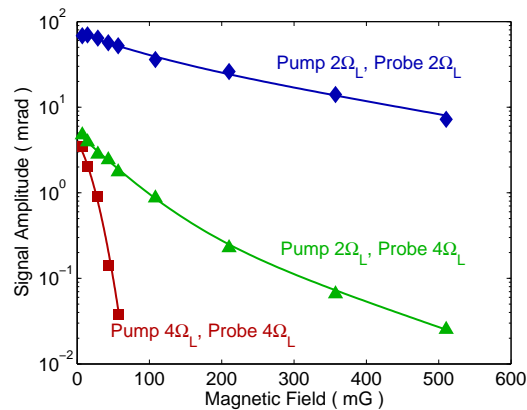


Fig. 2. Magnetic-field dependence of optical rotation amplitudes for quadrupole (blue diamonds), hexadecapole pumped with light modulated at $4\Omega_L$ (maroon squares), and hexadecapole pumped at $2\Omega_L$ (green triangles). The quadrupole and hexadecapole, pumped at $2\Omega_L$ decrease much more slowly with magnetic field compared to hexadecapole pumped at $4\Omega_L$. The solid lines are fits by ad-hoc functions.

repetition rate of $2\Omega_L/(2\pi) \approx 714$ kHz and 1/8 duty cycle. Significant beating of the signal is observed after the pulse sequence ends, resulting from NLZ (the effect of NLZ on nonlinear magneto-optical rotation is discussed in Ref. [21]). These beats are the time-domain manifestation of three closely spaced frequencies in the the optical rotation signal. Fits of the demodulated quadrupole signal indicate a splitting between adjacent frequencies of ≈ 72 Hz close to the calculated value of the NLZ splitting, $\delta_{NLZ} = 74.65$ Hz for this field. The overall exponential decay time ($\tau \approx 4.7$ ms) is determined by the relaxation of the PMs due to dephasing from collisions and magnetic-field inhomogeneities, and by residual probe-power broadening. Buried under the much larger quadrupole signal is also a hexadecapole signal producing modulation of the optical rotation at $4\Omega_L$. Unfortunately, due to nonlinearities in the detection electronics as well as those due to the interaction of atoms with a strong probe light [22], the large quadrupole signal leads to the presence of a “false hexadecapole” signal at $4\Omega_L$, and it is hard to distinguish the two contributions.

The solution implemented in the present work is to eliminate the quadrupole just before probing. To accomplish this, the pumping is separated into two stages. The first stage is the same as in the pumping scheme above: the atoms are pumped at $2\Omega_L$ for ≈ 1500 cycles. Then, the phase of the pumping is flipped by π radians (see inset in the bottom plot of Fig. 3). The quadrupole is now pumped orthogonally to its previous alignment and the resulting sum of orthogonal quadrupole moments leaves no net transverse alignment (the resulting doughnut shape, corresponding to longitudinal alignment that causes no optical rotation of the probe light, is shown inset at the bottom plot in Fig. 3). However, the hexadecapole produced before and after the phase flip is identical, so it continues to be pumped even after the phase flip. After ≈ 500 cycles, the quadrupole reaches a minimum and the pump is shut off. Figure 3 (bottom) demonstrates the phase-flip pumping scheme and the resulting signal. The quadrupole signal (not shown) is reduced by about a factor of 40 in this scheme, allowing for the reliable recovery of the signal due to the hexadecapole moment. The demodulated hexadecapole signal is a simple exponential decay ($\tau = 4.2$ ms), clearly demonstrating the absence of NLZ-induced beating. We expect that for the high-sensitivity magnetometry, it will be desirable to augment the signal-to-noise ratio of the hexadecapole signal by detecting fluorescence rather than optical

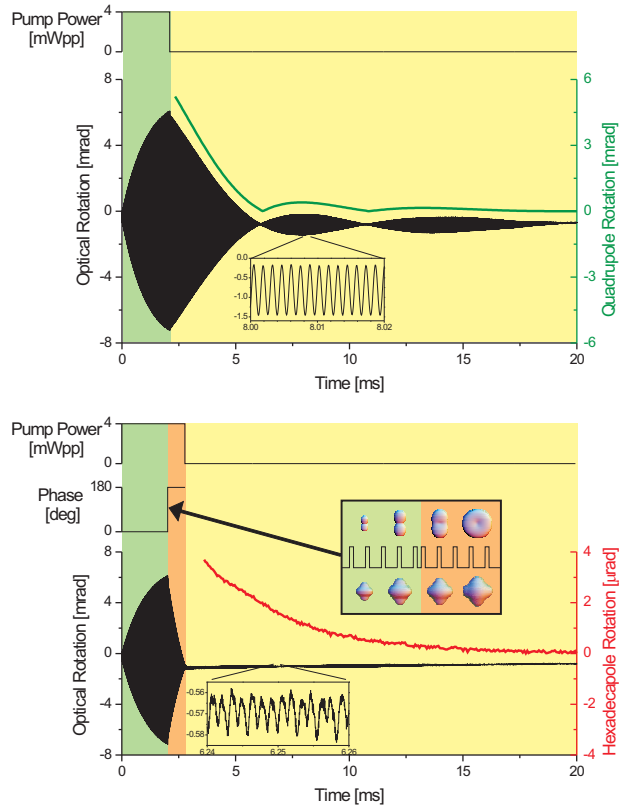


Fig. 3. Comparison of the demodulated quadrupole signal (top) without phase flip (see text) and of the hexadecapole signal obtained with phase flip (bottom). For the case of pumping without phase flip (top), the signal demodulated at $2\Omega_L$ is plotted alongside the raw optical rotation signal. The inset on the top plot is a magnification of the raw optical-rotation signal during a revival stage of the quadrupole-signal beats occurring due to the nonlinear Zeeman effect (NLZ). This signal on the bottom plot (with phase flip) is demodulated at $4\Omega_L$, and the resulting curve shows the absence of the beats related to NLZ. The inset on the right shows the details of the pumping pulses near the phase flip, along with the angular-momentum probability surfaces characterizing the ensemble at different stages of pumping. The magnetic field around which these surfaces precess is normal to the page.

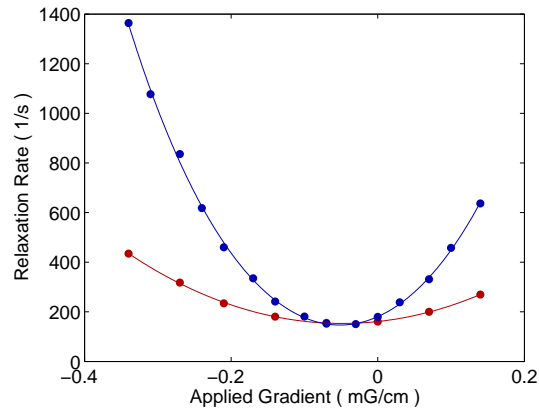


Fig. 4. The dependence of the observed relaxation rates for the quadrupole and hexadecapole signals on the magnetic-field gradient applied in the direction of the magnetic field. In both cases, pumping was with light pulsed at a repetition rate of $2\Omega_L/(2\pi)$ at $B \approx 108$ mG, and the relaxation was determined from the optical rotation after the pump light was shut off. Solid lines show fits to fourth-order polynomials; the ratio of curvatures near the vertex is consistent with the expected four times higher sensitivity of the hexadecapole to gradients [25].

rotation[23, 24, 15].

In an additional series of measurements, we studied the dependence of the quadrupole and hexadecapole optical-rotation signals on the magnetic field gradient. These measurements (Fig. 4) confirmed the expected (see, for example, Ref. [25]) four-times-higher sensitivity of the hexadecapole to field gradients compared to the quadrupole, underscoring the different physical character of these moments.

5. Conclusion

We have demonstrated a way to create and detect macroscopic hexadecapole polarization (corresponding to a four-quantum Zeeman coherence) in the geomagnetic field range. The amount of hexadecapole created at these fields was dramatically enhanced by pumping at $2\Omega_L$, the frequency associated with efficient production of the (lower-rank) quadrupole moment. Phase flipping allowed the elimination of the large quadrupole signal, unmasking the smaller hexadecapole signal. The resulting hexadecapole signal demonstrates the absence of beating associated with the nonlinear Zeeman effect. The NLZ-free hexadecapole signals are attractive for applications in optical magnetometry because the linear relation between the magnetic field and the spin-precession frequency is maintained over all magnetic fields. The demonstrated technique eliminates the major mechanism for heading error in atomic magnetometers, paving the way to a significant improvement in magnetic sensing accuracy using all-optical and mobile-platform sensors. Other possible applications of this technique include increased-capacity quantum memory devices employing selective optical addressing of higher-order coherences.

Acknowledgments

The authors acknowledge stimulating discussions with T. Karaulanov, and E. Corsini. This work has been supported by an ONR MURI program, NSF, and KBN grant # 1 P03B 102 30. S.P. is a scholar of the Foundation for Polish Science.